ФЕДЕРАЛЬНАЯ СЛУЖБА РОССИИ
ПО ГИДРОМЕТЕОРОЛОГИИ
И МОНИТОРИНГУ
ОКРУЖАЮЩЕЙ СРЕДЫ

РОССИЙСКАЯ АКАДЕМИЯ НАУК

ИНСТИТУТ ГЛОБАЛЬНОГО КЛИМАТА И ЭКОЛОГИИ

ПРОБЛЕМЫ ЭКОЛОГИЧЕСКОГО МОНИТОРИНГА И МОДЕЛИРОВАНИЯ ЭКОСИСТЕМ

Том XVIII

САНКТ-ПЕТЕРБУРГ ГИДРОМЕТЕОИЗДАТ 2002

УДК 551.510.42

Адрес: ул. Глебовская, д. 20Б, 107258 Москва, Россия
Институт глобального климата и экологии Росгидромета и РАН
Факс: (7 095) 1600831. Тел.: (7 095) 1691103

Все статьи данного сборника рецензируются.

Address: 20B, Glebovskaya str., 107258 Moscow, Russia
Institute of Global Climate and Ecology of Rosgidromet and RAS
Fax: (7 095) 1600831. Phone: (7 095) 1691103

All papers published in this book are reviewed.

Представлены работы, посвященные мониторингу и оценке ответной реакции экосистем на антропогенные воздействия регионального, континентального и глобального масштабов, в том числе на загрязнение атмосферы и изменения климата. Рассматриваются результаты экспериментальных исследований, а также математические модели экологических процессов.

Для климатологов, биологов и экологов широкого профиля.

The issues of monitoring and assessment of ecosystem response to anthropogenic impacts of regional, continental and global scale, in particular, to air pollution and climate change, are considered. The results of experimental studies as well as mathematical models of ecological processes are presented.

The book is of interest for climatologists, biologists and environmentalists.

П $\frac{1502000000\text{-}33}{069(02)\text{–}02}$

РЕАКЦИЯ ЭКОТОНА „ЛЕС — ТУНДРА" НА ИЗМЕНЕНИЕ КЛИМАТА

В. И. Харук[1], *С. Г. Шиятов*[2], *Е. Касишке*[3], *Е. В. Федотова*[1], *М. М. Наурзбаев*[1]

[1] РФ, 660036, Красноярск, Академгородок, Институт леса им. В. Н. Сукачева, kharuk@forest.akadem.ru

[2] РФ, 620144, Екатеринбург, ул. 8 Марта, Институт экологии растений и животных, stepan@ipae.uran.ru

[3] США, Гринбелт, Университет штата Мэриленд, MD

Реферат. Анализировалось влияние климатических трендов на экотон „лесотундра". Исследования выполнялись на ключевых участках „Ары-Мас" (самый северный в мире лесной массив, сформированный лиственницей: 72°28′ с. ш. — 101°40′ в. д.) и „Полярный Урал" (66°50′ с. ш. — 65°35′ в. д.), где переходная зона „лес — тундра" сформирована лиственницей с примесью ели. Использовались материалы спутниковой съемки системой CORONA (DISP), Landsat TM и аэрофотоснимки, а также материалы наземных обследований. Период наблюдений охватывал 1962—1998 гг. („Полярный Урал") и 1965—1991 гг. („Ары-Мас"). Установлено возрастание сомкнутости древостоев, а также продвижение лиственницы в зону тундры.

Ключевые слова. Глобальные изменения, экотон „лесотундра", граница леса.

FOREST — TUNDRA ECOTONE RESPONSE TO CLIMATE CHANGE

V. I. Kharuk[1], *S. G. Shiyatov*[2], *E. Kasishke*[3], *E. V. Fedotova*[1], *M. M. Naurzbaev*[1]

[1] Forest Institute, Academgorodok, 660036 Krasnoyarsk, Russia, kharuk@forest.akadem.ru

[2] Institute of Plant and Animal Ecology, 8 Marta street, 620144 Ekaterinburg, Russia, stepan@ipae.uran.ru

[3] University of Maryland, MD, Greenbelt, USA

Abstract. An analysis of climate trends impact on the forest — tundra ecotone was made. The studies were conducted on the key sites "Ary-Mas", the world most northward forest stand (72°28′ N/ 101°40′ E), and the "Polar Ural" (66°50′ N/65°35′ E). The forest — tundra ecotone is formed by larch in the "Ary-Mas" site and by larch

with admixture of spruce in "Polar Ural" site. The DISP (Declassified Intelligence Satellite Photography, taken by CORONA system), Landsat TM and airborne images together with on-ground data were involved in analysis. The periods of observations are 1963—1998 for the "Polar Ural" site and 1965—1991 for the "Ary-Mas" site. The increase in stand crown density and invasion of larch into tundra zone are determined.

Keywords. Global change, forest — tundra ecotone, tree line.

Introduction

There are several reasons for studying the responses of vegetation in Arctic and Subarctic regions to variations in climate. First, recent syntheses of surface weather observations clearly show the Arctic and Subarctic zones are areas where significant climate warming has occurred over the past half a century (Hansen et al., 1996), accompanied by increases in precipitation since 1950 (Maxwell, 1997). General circulation models predict that these regions will experience significant warming over the foreseeable future (Boer et al., 1992). Second, since the conditions in this region (short growing seasons, cold temperatures) are limiting to plant growth, any changes in climate are expected to result in changes in composition and patterns of photosynthesis of the ecosystems that occupy this region (Starfield, Chapin, 1996; Callaghan, Carlsson, 1997; Molau, 1997).

A number of different approaches have been developed for studying the response of the vegetation communities to variations in climate at high northern latitudes. At the broadest scale, inter- and intra-annual variations in the atmospheric concentration of CO_2 can be correlated to seasonal patterns of net primary production from terrestrial biomes (D'Arrigo et al., 1996; Randerson et al., 1999). These studies have shown that there is an overall correspondence between seasonal CO_2 fluctuations and patterns of vegetation detected through analysis of satellite imagery (D'Arrigo et al., 1996; Braswell et al., 1997; Myneni et al., 1997). The amplitude of the high-latitude CO_2 signature has been increasing over the past two decades, as a result of increased net primary production early in the growing season and heterotrophic respiration during the late growing season and winter (Randerson et al., 1999). These observations have provided the impetus behind many studies at global, regional and local scales to better understanding the factors contributing to seasonal variations in atmospheric CO_2 concentrations. Research includes modeling of processes responsible for the carbon exchange between the Earth's surface and the atmosphere at large scales (Kasischke et al., 1995; McGuire et

al., 1997; Field et al., 1998) and direct measurement of the exchange of CO_2 between the atmosphere and land surface at plot scales (Oechel et al., 1995; Zimov et al., 1996; Goulden et al., 1998; Zimov et al., 1999; Richter et el., 1999).

In terms of understanding the response of arctic/subarctic vegetation to climate change, the boreal forest-tundra ecotone represents a particularly important region because this is an area where tree species are growing at the limit of their range (Hustich, 1953). Different approaches used to monitor changes in vegetation characteristics in the forest-tundra ecotone include analysis of pollen in lake bottom sediments (Payette, Gagnon, 1985; Cwinar, Spear, 1991; MacDonald et al., 1993), analysis of plot data (Landhausser, Wein, 1993), and examination of tree rings (Briffa et al., 1998; Vaganov et al., 1996; Vaganov et al., 1999). These studies have shown that while over the longer term, variations in the growth and distribution of trees in this region are related to air temperature, over the shorter term, other factors (including disturbance, levels and patterns of precipitation and timing of snow cover) are also important.

In this paper, results of a study of the patterns of tree growth and distribution at two sites in northern Siberia that are located in the forest-tundra ecotone are presented. Evidence that the trees in these sites have undergone increased growth is presented in three forms: (1) analysis of plot data; (2) analysis of tree ring data; and (3) analysis of satellite imagery collected on two different dates (Declassified Intelligence Satellite Photography (DISP) and Landsat TM images).

Materials and methods

Study sites

Two test sites were selected for the studies: the Polar Ural and the Ary-Mas (Fig. 1). The Polar Ural site is located in the eastern foothills of the Ural Mountains, and just southeast of the Yamal Peninsula (66°50′ N/65°35′ E). The foothills in this region have an elevation of 1000 to 1300 m a. s. l. The study sites were located between the Kerdomanshor and Yengayu Rivers on gentle south-, southeast-, and southwest-facing slopes. The forest-tundra ecotone in this area occurs at an elevation of 300 m, with mountain tundra (shrub and lichen-moss tundra) existing up to elevations of 700—800 m, and cold deserts at higher elevations.

The mean annual temperature at the tree line is about −6°C (extreme minimum of −52°C and maximum of +32°C). Frosts can occur any time during the growing season, and permafrost underlies the entire area. The prevailing winds are from the west, with minimum speeds in the summer (5—6 $m \cdot s^{-1}$), and maximum in the winter (9—

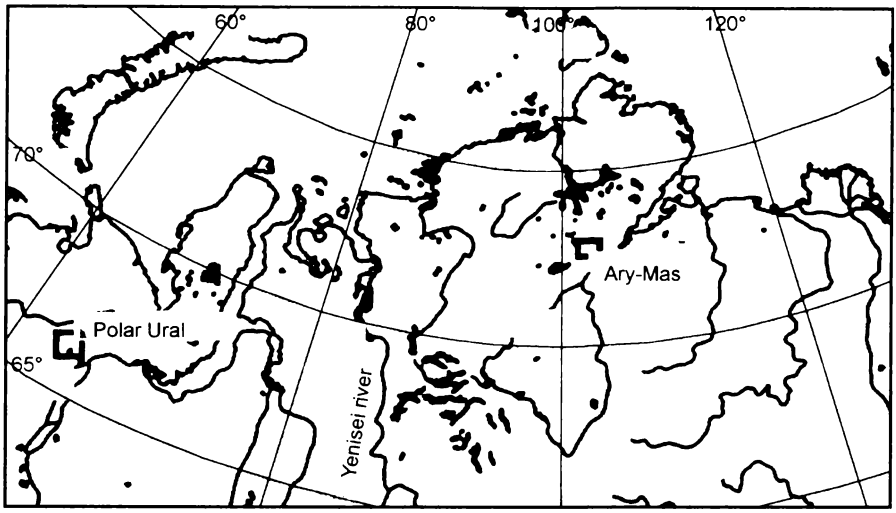

Fig. 1. The location of test sites.

10 $m \cdot s^{-1}$). During storms wind speed reaches 40 — 50 $m \cdot s^{-1}$. Annual precipitation is 500 — 600 mm, with the highest levels in September and the lowest in February and March. Snow and sleet comprise about 50 % of all precipitation. Snow depth is highly variable due to winds, terrain relief, stand structure and the distribution of stands over the site. Typical snow depth is 10—50 cm in tundra, 50 — 400 cm within tree stands and up to 540 cm in openings downwind of stands.

The soils on well-drained sites are podzols over sands and turf-podzol-gley over loams and clays. On poorly drained sites the soils are turf-bog-permafrost and turf-gley-permafrost types.

In the Polar Ural site the forest-tundra ecotone is formed by *Larix sibirica* with admixture of *Picea obovata* and *Betula tortuosa*. The average tree height is 10 m (the maximum is 16 m with a 20 to 30 cm diameter). At the upper limit trees are in a prostrate form. Shrubs in the forest understory include alder (*Alnus fruticosa*), polar birch (*Betula nana*) and several willow species (*Salix phylicifolia*, *S. lanata*, *S. glauca*). Shorter shrubs include *Vaccinium uliginosum* and *Empetrum nigrum*. The most representative moss and lichen species include *Pleurozium schreberi*, *Polytrichum strictum*, *Cladonia alpestris*, *Cladonia rangiferina* and *Nephroma arcticum*. Grass species are represented by *Carex* sp., *Equisetum* sp., *Polygonum* sp., *Sanguisorba* sp., *Solidago virgaurea*, *Veratrum* sp., and several *Gramineae* species. Vegetative cover is very patchy, which is typical for the forest-tundra ecotone. Forest cover is most developed in the shelters formed by relief (e. g., by moraines).

The Ary-Mas site is the world's northern most forested site (72°28′ N, 101°40′ E). In the language of the local native peoples, Ary-Mas means "Forest Island". Its length is about 25 km, and width ranges from 1 to 5 km. The forest stands occupy terraces on the banks of the Novaya River up to the elevations of 80 m a. s. l. To the north of the Ary-Mas site (up to 50 to 75 km) small stands of larch mainly in prostrate form exist in sheltered areas (creek valleys).

The mean annual temperature in this region is −14 °C. The mean January temperature is about −34 °C (absolute minimum −60 °C). The mean July temperature is +12 °C (maximum +25 °C). On the average, there are 260 days with sub-zero temperatures with an average growing season length of 60 days. The prevailing winds are from the west with an average speed about 5 $m \cdot s^{-1}$.

Annual precipitation is less than 300 mm, with about 80 mm occurring as snow during the winter. The number of days with snow cover is about 250. The snow depth averages 40 cm in open areas and more than 60 cm on the wind-protected areas. Within tree stands, the average snow depth depends on crown closure. For example, in stands with crown closure more than 0.3 drift depths reach 80 cm, whereas if this parameter is less than 0.3, the snow depth averages 50 cm. Snow drifting is an important factor in tree seedling survival because it prevents abrasion.

The soils of the Ary-Mas site are highly variable due to geomorphology and intensive cryogenic activities. Soils of areas with sparse tree stands are tundra-gley and tundra-humus-gley types. Within the sites where tree crown closure is more than 0.3, soils are taiga-permafrost-humus-gley and taiga-permafrost-turf-gley types. The depth of soil thawing is about 50 — 70 cm on areas with bare mineral soils, but only 10 to 30 cm in areas with moss cover.

Tree stands consist of *Larix gmelinii*. Tree heights are between 5 — 8 m (maximum of 11 m) with diameters of 10 — 14 cm (maximum of 25 cm). Cone production and seed fertility are poor. The shrub layer is formed by *Betula exilis*, *Ledum decumbens*, *Alnus fruticosa* and a mixture of different *Salix* sp. Typical grasses include *Carex ensifolia*, *Cassiope tetragona*, *Dryas punctata*. The dominant moss species are *Hylocomium splendens*, *Ptilidium ciliare*, *Aulacomnium turgidum*. Lichens are rare.

The annual temperatures from weather stations near the two test sites were analyzed, based on the data compiled by NASA's Goddard Institute for Space Studies (http://www.giss.nasa.gov). These data show that in the Polar Ural region there was a 2° to 3 °C drop in both annual and summer temperature between 1950 and the early 1970th, with a 1.5° to 2 °C rise in both temperatures between the early 1970th and 1998. The Ary-Mas region shows less variation, with the average

annual temperature increasing by 1.5 °C between the early 1960th and present and the summer temperature showing no variation (decrease or increase).

Data and methods

In the studies presented in this paper, we investigated changes in tree characteristics at the Ary-Mas site and changes in the location of the tree line and overall stand density in the Polar Ural site.

Field surveys in the Ary-Mas site were first conducted in 1969, when two sets of observations were made. First, a forest cover map was generated that contained the boundaries of six open woodland categories and twelve semi-closed woodland categories. Between 1969 and 1971, twelve survey plots (sizes ranging from 0.25 to 1.0 ha) were established in the different categories of forest. In each plot, a sketch map of the location of each individual canopy tree was created, and the characteristics of each tree were measured. Each plot was revisited in the summer of 1989-91 and the measurements were repeated. In the summer of 1991, cores were obtained from 25 of these trees for use in the analysis of tree rings. The tree rings data were analyzed using standard techniques (Vaganov et al., 1996).

To study changes in the tree line and stand characteristics, we used definitions for the forest — tundra transitions zones developed by Hustich (Hustich, 1953): (1) Tree line: the absolute maritime, polar or vertical limit of given species in tree form; (2) Species border: the limit attained by species irrespective of whether growth is prostrate, ascending, or tree like; (3) Sparse stand border: the boundary of stands where crown closure is 0.1; and (4) Stand border: the boundary of stands with crown closure more than 0.3.

The overall goal for the Polar Ural site was to determine if satellite imagery provides a basis for investigating the changes in the position of the tree line and for monitoring changing in crown closure. Two different satellite images collected over the Polar Ural site were used. The first image was collected in July 1968 by the CORONA satellite system operated by the U. S. National Reconnaissance Office. These data were declassified in 1995 and made available to the public. They are referred to as Declassified Intelligence Satellite Photographs (DISP). DISP imagery consists of black and white photographs with a ground resolution between 3 — 5 m. The second image was collected in July 1988 by the Landsat TM. While these data have a ground resolution of 30 m, they contain reflectance information from seven separate regions of the electromagnetic spectrum that can be used to discriminate different characteristics of the ground surface.

In the summers of 1960—1962, field surveys were conducted at the Polar Ural site to document the overall forest cover in this region. The approach used in this initial survey was designed to map the extent of sparse forest stands. During this survey, sketch maps were made to delineate: (1) boundary between tundra and sparse forest stands (e. g., crown closure more than 0.1) and (2) areas that had previously been occupied by forest but now contain tundra and dead trees.

In addition to forest stand boundary maps based on the 1960—1962 surveys, topographic map produced for the Polar Ural site in 1963 is used. The guidelines in marking the forest boundaries on these maps were based on a stand closure of 0.3.

In August of 1998, the Polar Ural site was revisited. The sets of 48 different plots were established for measurement of tree stand characteristics. These plots were used as a basis for the analysis of satellite imagery collected in 1988 and 1999. Approximately one half of the plots were located along the edge of the sparse-forest border based on the data collected in 1960—1962, while the other half were located along a transect perpendicular to this border. During 1998, information on tree crown closure, diameter, and the species composition and density of the understory was collected for each plot.

The first step in the analysis was geometrical correction of each satellite image. The DISP image was digitally scanned to allow the computer analysis of the data. Maximum likelihood classifier was applied as a classification method. In order to achieve a supervised classification of each image, a set of training areas was identified. For the DISP image, we assumed that some land categories (e. g., lakes, rivers, and bare grounds) did not change between dates of the field observations (1960—1962) and the dates of the satellite imagery acquisition (1965). The information from the 1960—1962 field surveys was used to identify sites of tundra and forests with crown closures more than 0.1 and the 1963 topographic map to identify sites where crown closure is more than 0.3. The ground surveys from 1998 were used as the training sites for the supervised classification of the 1988 Landsat TM imagery.

It is recognized that the overall precision of the approach used to classify the satellite imagery is sub-optimum, particularly for the 1988 Landsat TM image. However, the intent of this analysis was to evaluate the feasibility of satellite imagery to monitor changes in the tree line in this region.

For the Ary-Mas site remotely obtained data were presented by DISP dated by July 1965, and airborne image dated by July 1984 with the scale 1:15,000.

The kappa-statistic method was applied for the evaluation of mapping accuracy. This method allows comparing generated and referencing maps (Rosenfield, Fitzpatric-Lins, 1986). Kappa (κ) values less than 0.4 are considered as poor agreement, $0.4 < \kappa < 0.55$ as satisfactory, $0.55 < \kappa < 0.7$ as good, and $\kappa > 0.7$ as very good.

Results

1. The Polar Ural

An on-ground observation in 1998 has shown considerable changes in vegetation in comparison with 1962 data. Visually estimated, the stands crown closure has increased in 3 times. The tree diffusion into tundra was observed. The sparse stand borders ('0.1' crown closure) have shifted into tundra on 100 — 400 m, depending on the site.

1.1. Image analysis

DISP analysis. The DISP interpretation was based on the on-ground data taken in 1961—1962, and topographic maps. The image brightness as the single parameter was used for the DISP classification. Since this parameter depends on a number of factors (e. g., the presence and the type of vegetation, its projective cover, shadows, soil moisture, etc.), the correct division of the investigated land cover classes was highly problematic. For example, water in some lakes could be classified as high closure forest (due to its turbidity); some boggy areas could be misclassified as open woodlands; bushes along the creeks could be identified as a larch stands with crown closure more than 0.3. Fig. 2 shows means and standard deviations of the land cover classes signatures (for the training sites). The training sites correspond to the following on-ground classes: 1 — water, 2 — tundra, 3 — grass communities with shrubs admixture, 4 — shrub lands, 5 — larch stands with 0.1 — 0.2 crown closure, 6 — larch stands with crown closure not less than 0.3. The most difficult for detection (as in the case of Landsat TM image classification) was the class 5: it overlaps with class 4 (shrub lands) and class 6 (stands with crown closure 0.3 and more). Using above-mentioned training sites, the maximum likelihood classification was performed.

The result of classification is presented on Fig. 3. Mapping accuracy was evaluated for the classes 5 and 6, which are of the principal interest of this study. The analysis for the class 6 has shown a good agreement ($\kappa = 0.6$). For the class 5 $\kappa = 0.4$ (satisfactory); low κ values could be attributed to the small plots overlapping errors. Based on the data of Fig. 2 it is reasonably to suggest that for the other land cover

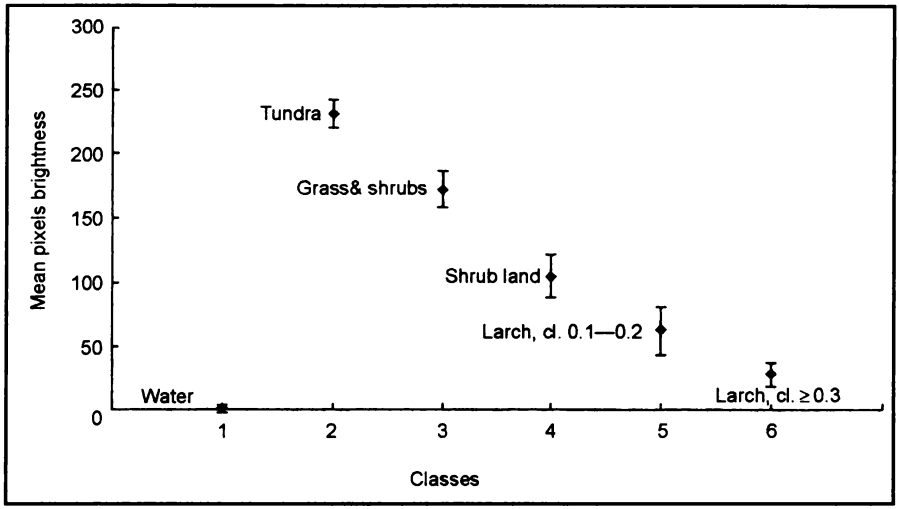

Fig. 2. The land cover classes signatures means and standard deviations (for the training sites) by DISP interpretation.

classes (1 — 4) the accuracy of classification not worse than for the class 6 at least.

The other approach for classification, the parallelepiped classification (Richards, 1993) was also performed. For this, the whole interval of the image brightness was divided into the non-crossing parts. The result of this classification was compared with the result of the maximum likelihood classification. In the Table 1 error matrix is presented for comparison of two classification methods (rows — numbers of pixels of the whole image in every of the parallelepiped derived classes, columns — the same for the maximum likelihood derived classes). The good consistency between these methods is observed: the number of points differs on 7 — 8 % only in the worst cases. In addition, the κ values have shown an excellent agreement (overall $\kappa = 0.96$).

Landsat TM image analysis. The training sites include the following land cover classes: 1 — water bodies; 2 — stony sites; 3 — stony-lichen tundra; 4 — lichen-shrub tundra; 5 — shrub lands; 6 — larch stands with crown closure less than 0.1; 7 — larch stands with crown closure 0.1 — 0.2; 8 — larch stands with crown closure 0.3 — 0.4; 9 — larch stands with crown closure 0.5 — 0.6; 10 — larch stands with crown closure 0.7 — 1.0. The number of classes is higher than in DISP analysis due to evident advantages of multispectral data.

Two basic methods were applied to evaluate the different TM channels separability: (1) the method described by Van Genderen et al.

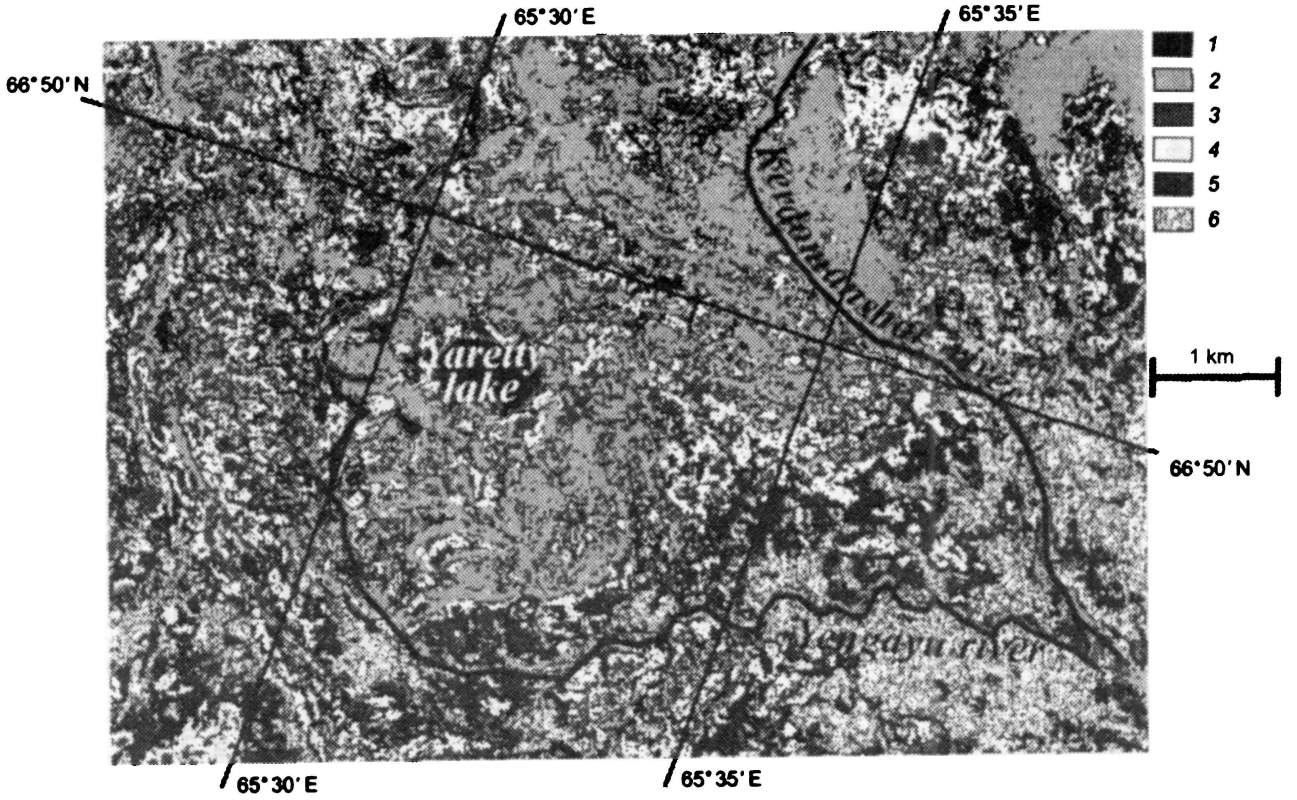

Fig. 3. The sketch-map of Polar Ural test site (DISP data).

1 — water, *2* — tundra, *3* — grass communities with admixture with shrubs, *4* — shrub lands, *5* — larch stands with 0.1—0.2 crown closure, *6* — larch stands with crown closure ≥ 0.3.

Table 1

Error matrix for comparison of maximum likelihood and parallelepiped classification methods for the Polar Ural study site (rows: numbers of pixels in the parallelepiped derived classes, columns: numbers of pixels in the maximum likelihood derived ones)

	Class 1[1)]	Class 2[2)]	Class 3[3)]	Class 4[4)]	Class 5[5)]	Class 6[6)]	Total
Class 1[1)]	51 517	0	0	0	0	0	51 517
Class 2[2)]	0	115 997	8 056	0	0	0	124 053
Class 3[3)]	0	0	350 649	36 313	0	0	386 962
Class 4[4)]	0	0	0	452 878	0	0	452 878
Class 5[5)]	0	0	0	0	350 897	0	350 897
Class 6[6)]	0	0	0	0	0	219 652	219 652
Total	51 517	115 997	358 705	489 191	350 897	219 652	1 585 959

[1)] Water.
[2)] Tundra.
[3)] Grass communities with shrubs admixture.
[4)] Shrub lands.
[5)] Larch stands with 0.1 — 0.2 crown closure.
[6)] Larch stands with crown closure ≥ 0.3.

(Van Genderen et al., 1978), and (2) Jeffries — Matusita (JM) distance (Richards, 1993). According the first method, the table of class signatures of the above-mentioned classes was generated (Table 2). As a measure of the degree of overlap between two classes was used a value $r = (x_1 - x_2)/(\sigma_1 + \sigma_2)$, where x_1, x_2 — mean values, σ_1, σ_2 — standard deviations of two classes signatures.

Table 2 shows that the channels 1, 2 and 3 (visible part of the spectrum) are poor in the land cover class's differentiation, since the values of the signatures are overlapped. Infrared channels are good for water bodies' detection. Channels 4, 5 and 7 are valid for stony area detection, and channel 7 for shrub land detection. The detection of the principal classes (larch stands) is not trivial task.

Classification accuracy is shown in the error matrix (Table 3). The stratified random sampling for the pixel selection was applied. The minimum sample size was determined as sixty test pixels within each class to ensure that the error matrix is an accurate reflection of the performance of the classification (Van Genderen et al., 1978). The rectangular windows containing mainly the points of given class were cut off from the image; it should be noted that due to the mosaic pattern of the analyzed territory the areas within windows were not completely homogenous. Then, based on ground truth data, these sixty test pixels were identified. It should be noted that in the Table 3 class 9 is the sum of classes 9 and 10 of the Table 2. This was made for

Table 2

The statistical characteristics (mean/st. deviation) of class signatures for Landsat derived classes of surface

	Landsat channel 1	Landsat channel 2	Landsat channel 3	Landsat channel 4	Landsat channel 5	Landsat channel 6	Landsat channel 7
Class 1[1)]	69.9/2.39	22.3/1.64	19.9/1.66	10.7/1.68	6.7/1.90	106/1.52	3.6/1.57
Class 2[2)]	85.1/5.61	30.0/2.79	33.8/4.28	26.9/4.87	37.7/9.97	111/2.51	21.2/5.90
Class 3[3)]	81.4/2.33	28.9/1.21	34.2/2.26	39.9/3.44	63.8/2.51	115/1.26	33.9/2.47
Class 4[4)]	81.8/2.51	29.3/1.26	34.2/2.32	50.28/2.99	79.4/2.09	120/0.72	38.3/2.12
Class 5[5)]	85.2/2.37	29.3/1.07	33.1/1.82	37.0/9.12	83.0/2.51	116/0.74	49.7/3.48
Class 6[6)]	75.5/2.48	26.5/1.10	27.9/1.07	60.0/1.49	73.2/1.74	115/0.81	29.1/1.56
Class 7[7)]	77.5/3.19	27.0/1.33	29.8/1.33	56.2/5.87	78.2/1.91	121/1.35	34.7/2.71
Class 8[8)]	72.4/1.67	24.9/0.93	24.3/1.21	69.9/6.48	71.1/1.88	119/1.02	26.5/2.57
Class 9[9)]	70.3/1.62	23.8/0.80	22.2/0.97	75.3/6.88	63.2/2.27	115/0.96	21.1/1.64
Class 10[10)]	69.2/1.67	22.4/0.64	21.1/0.99	62.5/4.23	57.0/3.05	114/1.62	19.8/1.86

[1)] Water bodies.
[2)] Stony sites.
[3)] Stony-lichen tundra.
[4)] Lichen-shrub tundra.
[5)] Shrub lands.
[6)] Larch stands with crown closure less than 0.1.
[7)] Larch stands with crown closure 0.1 — 0.2.
[8)] Larch stands with crown closure 0.3 — 0.4.
[9)] Larch stands with crown closure 0.5 — 0.6.
[10)] Larch stands with crown closure 0.7 — 1.0.

Table 3

Error matrix of maximum likelihood classification for Polar Ural study site

Image classes	Map classes								
	Cl. 1 [1]	Cl. 2[2]	Cl. 3[3]	Cl. 4[4]	Cl. 5[5]	Cl. 6[6]	Cl. 7[7]	Cl. 8[8]	Cl. 9[9]
Class 1[1]	54								
Class 2[2]	6	57							
Class 3[3]		1	59						
Class 4[4]			5	39					
Class 5[5]			3	3	41		1		
Class 6[6]			1	3		58		6	
Class 7[7]			13				49		
Class 8[8]				16				37	2
Class 9[9]									60

[1] Water bodies.
[2] Stony sites.
[3] Stony-lichen tundra.
[4] Lichen-shrub tundra.
[5] Shrub lands.
[6] Larch stands with crown closure less than 0.1.
[7] Larch stands with crown closure 0.1 — 0.2.
[8] Larch stands with crown closure 0.3 — 0.4.
[9] Larch stands with crown closure 0.5 — 1.0.

two reasons: (1) the detection of these classes is not principal for this study, and (2) it improves the level of classification.

Table 3 data shows that the errors are maximal for the following classes: 4 (lichen-shrub tundra); 5 (shrub lands); 7 and 8 (larch stands with crown closure 0.1 — 0.2 and 0.3 — 0.4, correspondingly).

The second applied algorithm for the Landsat-TM channels validity for land cover classification was the Jeffries — Matusita (JM) distance (Richards, 1993). The JM distance between a pair of spectral classes is defined as

$$JM_{ij} = \int_x \left\{ \sqrt{p(x|\omega_i)} - \sqrt{p(x|\omega_j)} \right\}^2 dx, \qquad (1)$$

where $\sqrt{p(x|\omega_i)}$ — a probability of finding a pixel from class ω_i at the position x. For normally distributed classes this becomes

$$JM_{ij} = 2(1 - e^{-B}), \qquad (2)$$

in which

$$B = 1/8(\mathbf{m}_i - \mathbf{m}_j)^t \left\{ \frac{\Sigma_i + \Sigma_j}{2} \right\}^{-1} (\mathbf{m}_i - \mathbf{m}_j) + 1/2 \ln \left\{ \frac{\left| (\Sigma_i + \Sigma_j)/2 \right|}{|\Sigma_i|^{1/2} |\Sigma_j|^{1/2}} \right\}, \qquad (3)$$

where i and j — the two signatures (classes) being compared, Σ_i — the covariance matrix of signature i, $\mathbf{m}_i$ — the mean vector of signature i, $|\Sigma_i|$ — the determinant of Σ_i.

According to this, the most informative is the set of the signatures for which the sum of the JM distance for the given classes is maximal. The calculated JM distances showed, that the most informative is the pair of 3rd and 5th channels (0.63 — 0.69 and 1.55 — 1.75 mkm, correspondingly). Also the channel 6 (10.4 — 12.5 mkm) and Normalized Difference Vegetation Index (NDVI) showed high JM value. The values of NDVI are derived from reflectance measurements in the red (L_{red}) and infrared (L_{Ired}) portions of the electromagnetic spectrum as follows:

$$\text{NDVI} = (L_{Ired} - L_{red})/(L_{Ired} + L_{red}). \quad (4)$$

For Landsat TM those are the data from third and fourth bands correspondingly.

The differentiation of the main land cover classes is shown on the Fig. 4 (in the 3 — 5 channels coordinates on the Fig. 4A, and in the channel 6 — NDVI coordinates on the Fig. 4B). For every class were chosen five pixels in a random way on the image. The brightness values of Landsat TM bands and NDVI for every pixel were taken as coordinates. These graphs show that seven of nine land cover classes could be divided using information in these channels plus NDVI (zones of points for seven classes are not overlapped). The most complicated classes are the lichen tundra and larch stands with crown closure less than 0.1. This is understandable since backgrounds of the larch stands with low closure are often lichens. Two classes, rocks and larch with crown closure less than 0.1, which are poorly divided in the 3 — 5 channels, are separated in the NDVI — channel 6 coordinates due to the thermal differences of these land cover classes. Meanwhile in these coordinates water and grass-bush tundra are poorly differentiated. This could be due to the fact that the last class is often presented by wetlands.

The classification of Landsat TM image was made by maximum likelihood method, and all seven TM channels were involved. The derived sketch-map is presented on Fig. 5. The following land cover classes were mapped: *1* — water; *2* — rocks; *3* — tundra; *4* — grass communities; *5* — shrubs; *6* — stands with crown closure less than 0.1; *7* — stands with crown closure 0.1 — 0.2; *8* — stands with crown closure 0.3 — 0.4; *9* — stands with crown closure 0.5 and more. It should be noted that the rivers are marked mainly by red color (class 2: stones) on the original colour sketch-map since rivers are shallow and surrounded by wide stony riverbanks.

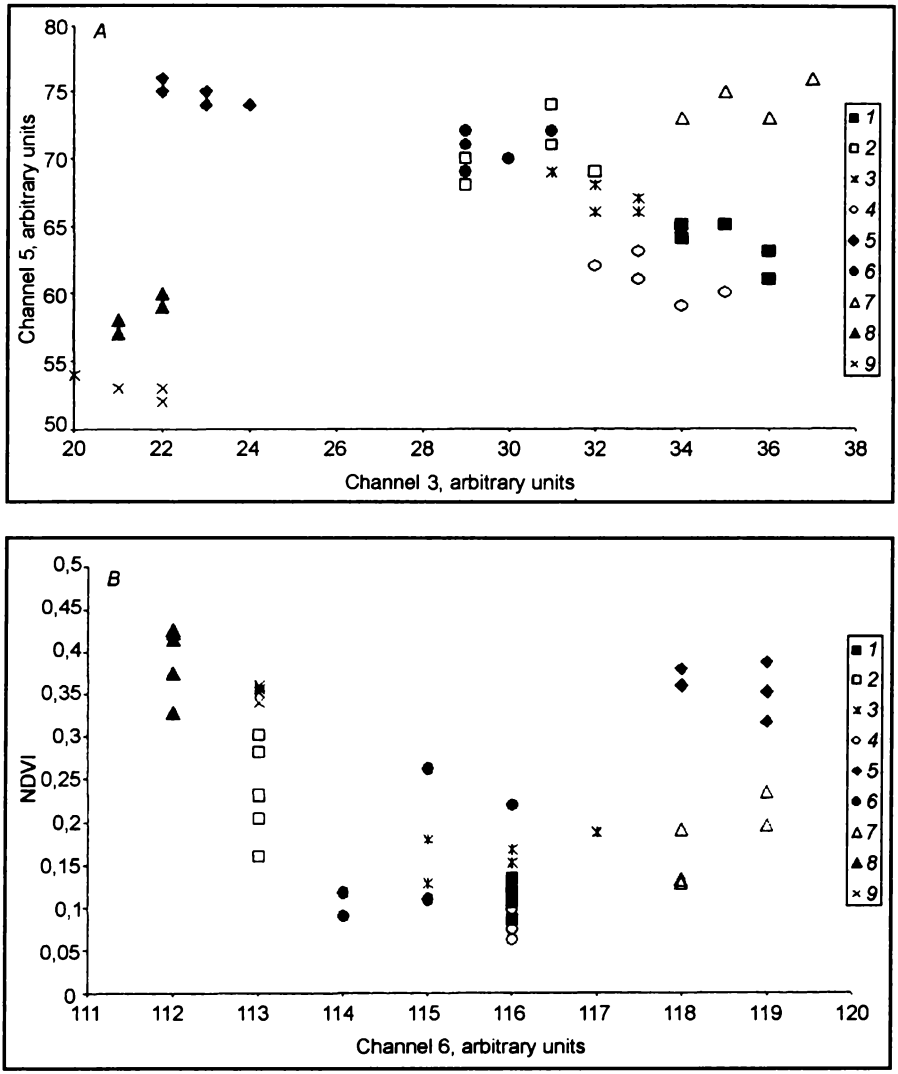

Fig. 4. The Landsat-TM channel validity for land cover classes separation in 'channel 3 — channel 5'(*A*) and 'channel 6 — NDVI' (*B*) coordinates.

Land cover classes: *1* — water, *2* — rocks, *3* — tundra, *4* — grass communities, *5* — stands with crown closure < 0.1, *6* — stands with crown closure 0.1—0.2, *7* — stands with crown closure 0.3—0.4, *8* — stands with crown closure 0.5—0.7, *9* — stands with crown closure ≥ 0.8.

The classification accuracy analysis shows that the most complicated case is the differentiation of the stands with low values of the crown closure (classes 5, 6 and 7; Table 3). This is due to the fact that

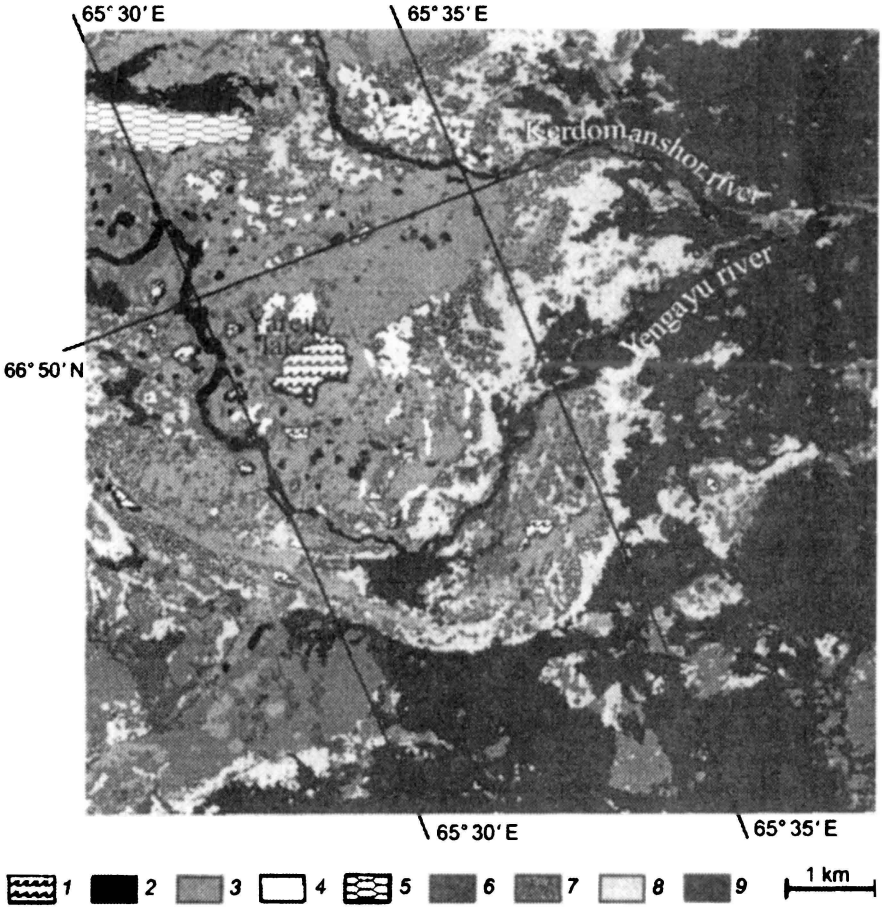

Fig. 5. The sketch-map of the Polar Ural test site (Landsat-TM data).
1 — water, *2* — rocks, *3* — tundra, *4* — grass communities, *5* — stands with crown closure < 0.1, *6* — stands with crown closure 0.1—0.2, *7* — stands with crown closure 0.3—0.4, *8* — stands with crown closure 0.5—0.7, *9* — stands with crown closure ≥ 0.8.

classes 6 and 7 are actually a dense shrub lands (mainly formed by *Betula nana*) with spectral characteristics similar to the medium-closed (0.3—0.4) larch stands (class 8). Actually, the large proportion of the class 8 includes dense shrubs (as lower layer).

The time series of stand borders is presented on Fig. 6. The dynamics of the areas with different crown closure is presented in Table 4.

These data shows increasing of the territory proportion with higher stands crown closure. Namely, the stands territory with crown closure more than 0.3 in 1968 was about 235 % of territory in 1963, and more than 500 % in 1988. During the period between 1968 and

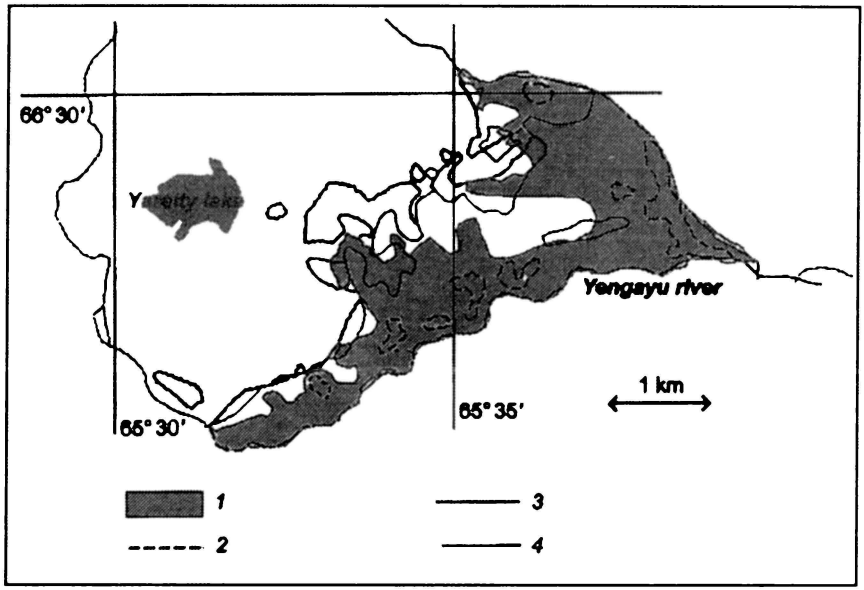

Fig. 6. The time series of larch stand borders in Polar Ural test site.
1 — stands with crown closure 0.1, 1960; *2* — stands with crown closure 0.3 and more, 1960; *3* — stands with crown closure 0.1, 1988; *4* — stands with crown closure 0.3 and more, 1988.

1988 the territory of stands with crown closure more than 0.1 practically has not changed. Partly this could be attributed to the difficulties of differentiating between shrub lands and larch stands with low density. On the other hand, the similar values of the total areas covered with larch stands with crown closure more than 0.1 derived from the DISP (7.0 km^2) and Landsat TM (7.08 km^2) images show the consistency of the data obtained. Table 4 data provides the evidence that during the quarter of century (1963 — 1988) the increase of the larch stand crown closure (as response to climate change) was observed. The involvement into analysis of the updated images (e. g., Landsat-7) allows to reconstruct the temporal dynamics for more than three decades.

Table 4

The dynamics of the areas with different crown closure (between the Yengayu and Kerdomanshor rivers)

Crown closure	Maps 1963	DISP 1968		Landsat-TM 1988		
	Area, km^2	Area, km^2	Percent of 1963	Area, km^2	Percent of 1963	Percent of 1968
< 0.1	5.5	7.0	127	7.08	129	101
0.1—0.2		4.7		2.04		
0.3—1.0	0.98	2.3	235	5.04	514	220

2. Ary-Mas

2.1. Image analysis

The fragments of remotely obtained data for Ary-Mas are presented on Fig. 7 *A* (1965, DISP) and Fig. 7 *B* (1984, airborne image). The airborne image was modified: its resolution was degraded to the resolution of the DISP image. Both images were processed to evaluate the areas with the typical crown closure; as the reference the test area 5 with crown closure about 0.15 was chosen (Table 5). The result of the image analysis (within the boxes on Fig. 7 *A*, *B*) is presented on the Fig. 7 *C*, *D*. The area within the box with stand closure 0.15 and more has increased since 1965 for 3.6 ha, or for 15 %.

2.2. On-ground data analysis

The results of the forest inventory data analysis for the Ary-Mas site is presented in Table 5.

The calculations of mean stem volume increment for the period between measurements were made on the following basis. All trees were divided in three groups:

1. The trees of the first measurements group (1969—1971).
2. The trees of the second measurements group (1989—1991).
3. The trees which were in the first measurements but absent in the second one. This group includes cut, broken dead, wind-fallen trees. The regeneration (the trees with the height less than 2 m) was not considered. The mean diameter was calculated by the following formula:

$$d_m = 2\sqrt{(\sum LG_i/(\pi N))}, \tag{5}$$

where $G_i = (d_i)^2\pi/4$, d_i is the diameter of i-th tree, N is the number of trees on the test area.

The mean tree's height was determined by formula

$$h_m = \sum(h_i G_i)/\sum G_i, \tag{6}$$

where h_i is the height of i-th tree. The stem volume per hectare was determined by formula

$$M = \sum G_i FH, \tag{7}$$

where F is the form factor and FH is a value dependent on the mean tree's height (Abaimov et al., 1997).

Table 5

The forest inventory data for the Ary-Mas site

Test site	Soil drainage	N/ha	N/ha mort	d_m, cm			h_m, m			M, m³/ha			P_m
				'69—'71	'89—'91	mort	'69—'71	'89—'91	mort	M_1	M_2	M_{mort}	
1	Poor	532	56	7.84	8.54	8.37	4.72	4.92	5.91	6.89	8.53	0.98	1.7
2	Moderate	592	184	7.27	9.23	5.54	5.50	6.26	4.53	7.25	12.97	1.14	3.4
3	Well	142	118	5.70	6.41	4.44	3.89	4.39	3.50	0.87	1.19	0.40	3.5
4	Poor	864	44	9.03	9.67	4.35	6.83	6.81	3.83	19.34	22.13	0.15	0.7
5	Moderate	364	52	9.18	10.7	8.17	5.41	5.68	5.54	7.16	9.96	0.80	2.0
6	Well	173	103	3.50	4.67	2.57	3.11	3.68	2.84	0.34	0.67	0.10	4.3
7	Well	572	360	7.08	8.66	6.38	5.57	6.05	5.92	6.73	10.66	3.66	4.4
8	Moderate	142	138	3.21	4.30	3.69	3.17	3.67	3.64	0.24	0.47	0.33	7.9
9	Well	128	72	4.17	5.27	3.29	3.59	4.06	3.21	0.39	0.67	0.13	3.9
10	Poor	332	48	8.82	9.70	8.92	5.55	5.87	5.33	6.03	7.72	0.88	1.9
11	Well	148	114	1.81	3.40	2.13	2.51	3.35	2.56	0.07	0.30	0.07	8.1
12	Well	720	128	5.24	6.92	4.45	4.50	4.75	4.60	3.97	7.32	0.52	3.4
									Mean:	4.94	6.88	0.76	2.3

Notes. N/ha is the number of trees per 1 ha; 'mort' is attributed to the dead portion of stand (in the 1989—1991 measurements); d_m is the mean tree's diameter (cm); h_m is the mean tree's height (m); '69 — '71, '89 — '91 are the datum of measurements (1969—1971 and 1989 — 1991, correspondingly); M, m³/ha is the stem volume per 1 ha; M_1, M_2 are the stem volumes in the first (1969 — 1971) and second (1989 — 1991) measurements; P_m is the mean stem volume increment (%) for the period between measurements (see equation 8). The soils were classified with respect to the drainage level.

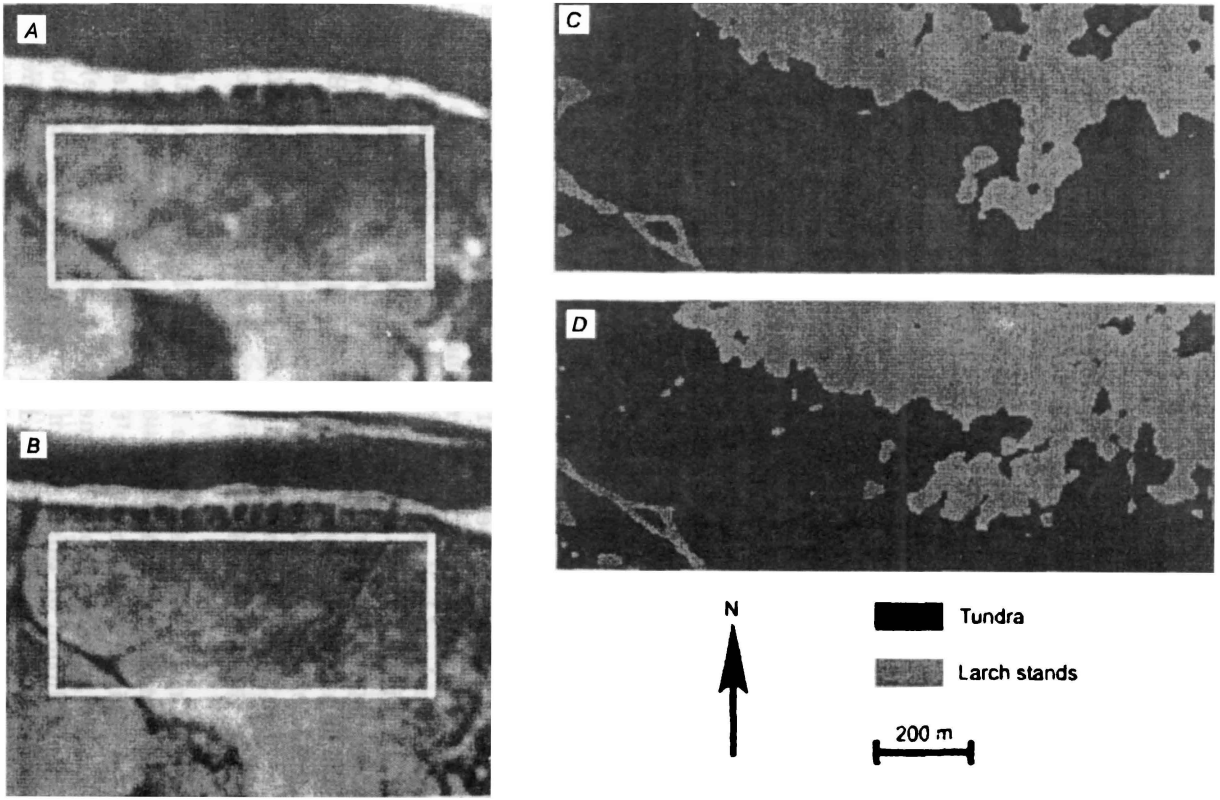

Fig. 7. The fragments of remotely obtained data for the Ary-Mas site.
A — DISP (1965), *B* — airborne image (1984), *C* and *D* — the results of the image analysis (within the boxes on Fig 7 *A*, *B* correspondingly).

The yearly mean stem volume increment was determined by "Pressler formula" (Antanaitis, Zagreev, 1981):

$$P_m = (M_2 - M_1 + M_{mort})/(M_2 + M_1) \cdot 200/n, \quad (8)$$

where M_1, M_2 are the biomass in the first (1969 — 1971) and second (1989 — 1991) measurements, n is a number of years between measurements (20 yr).

The Table 5 data show that during the period between first and second measurements the increasing of the stem volume (i. e. biomass) for the all test plots was observed. The average increase for two decades was about 2.7 $m^3 \cdot ha^{-1}$ ($M_2 - M_1 + M_{mort}$), or about 55 % (in comparison with M_1). The averaged per annual increase of biomass was about 0.13 $m^3 \cdot ha^{-1} \cdot yr^{-1}$), or 2.8 % per yr. The actual increment should be even bigger since the data on regeneration were not available.

The P_m values are highly varying (from 0.7 % to 7.9 %) for the different test plots. It was supposed that observed variations are connected with site conditions and age. The main measured site conditions were the stand crown closure, moss and lichen mat thickness and cover closure, and the depth of summer soil thawing. The regression analysis has shown that relation is significant ($p = 0.1$) only for the depth of soil thawing. For the moss and lichen cover closure, the p level was only 0.4 and even smaller for the other parameters. It should be noted that, generally speaking, low levels of reliability are typical for the data of forest-tundra zone because of its mosaic nature. Nevertheless, the positive correlation of above mentioned parameters with biomass increase has and evident ecological meaning. The depth of the soil thawing is critically important for the root function, and this parameter directly depends on the moss and lichen cover closure. Moreover, closed lichen and moss cover complicates seed germination. Both of these parameters, as well as biomass increase, are maximal for sparse open stands on the border with tundra (sites No. 3, 6, 8, 9, 11). In the other words, this result supports the hypothesis of tree invasion into tundra.

The above-made conclusions are based on the assumption that before the first measurements (1969 — 1971) the average increment was about zero. This assumption couldn't be proved by inventory data. On the other hand, dendrochronology methods (tree ring structure) could be used for solution of this problem by prolongation of the observations period. For this purpose the radial growth increment of the samples was analyzed. Figure 8 presents a plot of indices of tree ring width (ITRW) for trees taken from the Ary-Mas site. For the period from 1948 to 1971 there is an overall decreasing trend in the tree ring

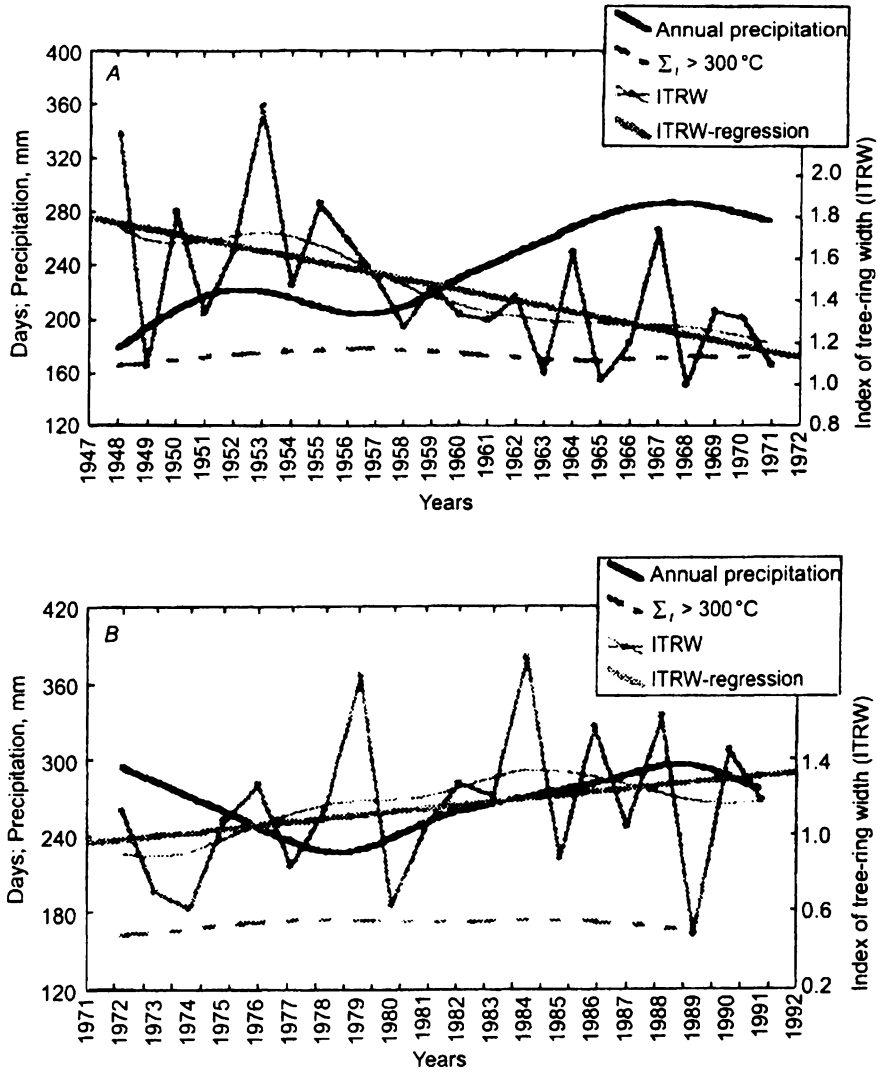

Fig. 8. The indexes of tree-ring width (ITRW) for the periods 1948—1991.
A — 1948—1971, *B* — 1972—1991.

width ($R = 0.54$ at $p < 0.05$), while from 1972 to 1991 there is an increasing in tree ring width ($R = 0.27$ at $p < 0.05$). The analysis of the weather data near this site shows that there was an overall increase in precipitation between the two periods, while temperatures remained constant. The tree ring widths were correlated with a variety of cli-

matic parameters, including cumulative degree-days above zero greater than 300 °C (where 300 °C is assumed to be the beginning of the growing season). It was found that a significant level of the variation in the tree ring widths was explained by a combination of winter precipitation and cumulative degree-days above 300 °C ($R = 0.79$ at $p < 0.001$).

The increases in tree growth between 1972 and 1991 inferred from the tree-ring data are also reflected in the plot data collected at the Ary-Mas site. These data show increasing in mean stem volume ranging from 0.7—8.1 $\% \cdot yr^{-1}$, with an average of 2.3 $\% \cdot yr^{-1}$. Figure 8 considers the trees that were surveyed in 1969—1972 and factor in tree mortality but do not include seedlings that were established during the 1969—1991 period.

Discussion

The above-described changes of forest-tundra ecotone could be attributed to the (1) earlier beginning of the vegetation growth and (2) increase of winter precipitation. The first factor evidently prolongs of the vegetative period, increase of cone/regeneration production and regeneration surviving. The last is especially important since young trees are most sensitive to the damage. The critical point of their life is the time when saplings becomes higher than the zone sheltered by shrubs and snow cover. Theirs stems and branches face winter desiccation and snow abrasion. This caused seedling mortality or appearance of prostrate forms. The increase of winter precipitation promotes seedling survival due to higher snow pack. Precipitation could also promote larch expansion into the zone of relatively dry soils (with better drainage). Water in the forest-tundra ecotone could limit a tree growth. For example, the level of precipitation on the Ary-Mas site (less than 300 mm) corresponds to semi-desert area. Larch forests exist due to the low level of evaporation (50 — 100 mm), and high efficiency of water use that is the larch advantage (Kloeppel et al., 1998). The trend to occupy areas with relatively dry conditions was noted for both, the Polar Ural and the Ary-Mas sites. For example, in the Ary-Mas site the increase of stand's productivity is more significant on the relatively dry plots with moderate and well drainage (Table 5). On the other side, the level of soil melting on those plots is higher; i. e. deeper soil horizons are available for roots. In addition, in case of spring drought the soil water stored since last growing period is higher in such plots. We should state that this problem needs more investigations.

Vegetation follows the climatic changes with the lag: during warming period the tree line is behind its potential climatic border,

and *vice verse* during cooling period. The first is due to the limitation in the tree regeneration (germination capacity, seeds spreading, seedlings survive), the second is due to the higher resistance of mature trees to the environmental conditions. These causes "phase shift" between stand closure/productivity and tree regeneration. The analysis of the age structure of the Ary-Mas site stands shows the 10 — 15 yr. delay between maximum of increment growth and establishment of new generation of trees.

Trees propagate into the tundra by two mechanisms. (1) "Tree diffusion" from the "main wall of stand" to the distance corresponding to the radius of seeds sedimentation (30 — 60 m). After about 30 years (the period of tree maturation) the other wave of regeneration is expected. (2) From the single trees or prostrate forms of larch; these sources of seeds could be on the distance up to 1 — 3 km from the "mother stand". The input of birds and small animals into this process should be also elucidated. The warming promotes transformation of the prostrate form of larch into the tree form. The prostrate forms of larch often consist of several stems ("bush-like" form), since larch ability of regenerating by layering. As response to climate change these "bush-like" larch becomes a normal tree, forming "clusters" with several individual trees.

Consequently, there are two main types of the forest-tundra borders: diffuse and mosaic.

Tree propagation due to extension of "mosaic" elements could considerably increase the total speed of tree propagation into tundra, since seeds fertility in the forest-tundra zone is low (about 5 — 7 %) and the radius of the seeds dispersion is limited.

The presented data describes the phenomena of forest-tundra ecotone response to climate changes. It manifested in the tree expansion into tundra, increase of stand crown closure and biomass.

This is shown for two sites of circumpolar zone with distance between them about 1600 km. Since the test sites are far from the industrial centers (more than 600 km), side effects (like fertilization) are excluded. Earlier reported data for the Northern Hemisphere (Myneni et al., 1997) has esteemed the increase of the productivity on about 10 % during 1980—1990 decade. That study was based on the satellite data only. According to our estimation, productivity of forest-tundra ecotone during the same decade increased about 28 %. This could be considered as one of the first evidence of the boreal vegetation response to the climate trends. The next step in these studies is the prolongation of the time series of observations by using the Landsat-7 data. It allows reconstructing the temporal changes during more than three decades.

The results presented in this paper are consistent with observations made in other studies. The relationship between variations in

climate and tree-ring width data in tree line sites has been shown to be complex. While these studies show there is an overall correlation between summer temperature and tree growth, other factors, as a timing of spring snow melt, are particularly important (Vaganov et al., 1999). The tree-ring data from the Ary-Mas site show that the levels of winter time precipitation and growing degree-days explain a high percentage of the variations in tree growth. The plot data from the Ary-Mas site show that there has been a significant increase in tree volume during the 1970th and 1980th, consistent with the general trend in increasing of tree-ring width for this site over the same period.

Studies of changes in tree characteristics at tree lines in Northern Canada have shown that the primary effect of climate warming has been on tree density, and that there have been only minor changes in the placement of the tree line (Payette, Gagnon, 1985). These observations are entirely consistent with the results from the Polar Ural site. Analysis of satellite data indicates there has been only a modest change in the border of the tree stands (stands with crown closure 0.1 and more), but a large increase in the area of stands with crown closure not less than 0.3. These results show the potential of using satellite imagery for monitoring variations in tree density at tree line sites in the Arctic.

Acknowledgment

This work was supported by RFFI grant 97-05-65664.

REFERENCES

Abaimov A. P., Bondarev A. I., Zyryanova O. A., Shitova S. A. 1997. Subarctic forests of Krasnoyarsk region. — Novosibirsk, Nauka, 206 p. (In Russian).

Antanaitis V. V., Zagreev V. V. 1981. The forest growth. — Moscow, Lesnaya promyshlennost, 200 p. (In Russian).

Ary-Mas. 1978. — Leningrad, Nauka, 190 p. (In Russian).

Boer G. J., McFarlane N., Lazare M. 1992. Greenhouse Gas-induced Climate Change Simulated with the CCC Second-Generation General Circulation Model. — J. Clim., v. 5, p.1045 — 1077.

Braswell B. H., Schimel D. S., Linder E., Moore B. III 1997. The Response of Global Terrestrial Ecosystems to Interannual Temperature Variability. — Science, v. 278, p. 870 — 872.

Briffa K. R., Schweingruber F. H., Jones P. D., Osborn T. J., Shiyatov S. G., Vaganov E. A. 1998. Reduced sensitivity of recent tree-growth to temperature at high northern latitudes. — Nature, v. 391, p. 678 — 682.

Callaghan T. V., Carlsson B. A. 1997. Impacts of Climate Change on Demographic Processes and Population Dynamics in Arctic Plants. — In: Global Change and Arctic Terrestrial Ecosystems. — Springer-Verlag, New York, p.129 —152.

Cwynar L. C., Spear R. W. 1991. Reversion of forest to tundra in the central Yukon. — Ecology, v. 72, p. 202 — 212.

D'Arrigo R., Jacoby G. C., Fung I. Y. 1996. Boreal forest and atmosphere — biosphere exchange of carbon dioxide. — Nature, v. 329, p. 321 — 323.

Field C. B., Behrenfeld M. J., Randerson J. T., Falkowski P. 1998. Primary Production of the Biosphere: Integrating Terrestrial and Oceanic Components. — Science, v. 281, p. 237 — 240.

Goulden M. L., Wofsy S. C., Harden J. W. et al. 1998. Sensitivity of Boreal Forest Carbon Balance to Soil Thaw. — Science, v. 279, p. 214 — 217.

Hansen J., Ruedy R., Sato M., Reynolds R. 1996. Global surface air temperatures in 1995: Return to pre-Pinatubo levels. — Geophys. Res. Letters, v. 23, p. 1665 — 1668.

Hustich I. 1953. The boreal limits of conifers. — Arctic, No. 6, p. 149 — 162.

Kasischke E. S., Christensen N. L. Jr., Stocks B. J. 1995. Fire, global warming and the carbon balance of boreal forests. — Ecol. Appl., v. 5 (2), p. 437 — 451.

Kloeppel B. D., Gower S. T., Trechel I., Kharouk V. I. 1998. Foliar carbon isotope discrimination in Larix species and sympatric evergreen conifers: a global comparison. — Oecologia, v. 114, p. 153 — 159.

Kruchkov V. V. 1967. Forest-tundra specificity causes. — In: Forest-tundra vegetation. — Leningrad, Nauka, p. 5 — 11. (In Russian).

Landhausser S. M., Wein R. W. 1993. Postfire vegetation recovery and tree establishment at the Arctic treeline: climate change — vegetation response hypotheses. — J. Ecol., v. 81, p. 665 — 672.

MacDonald G. M., Edwards T. W. D., Moser K. A., Pienitz R., Smol J. P. 1993. Rapid response of treeline vegetation and lakes to past climate warming. — Nature, v. 361, p. 243 — 246.

Maxwell B. 1997. Recent Climate Patterns in the Arctic. — In: Global Change and Arctic Terrestrial Ecosystems. — Springer-Verlag, New York, p. 21 — 46.

McGuire A. D., Melillo J. M., Kicklighter D. W. et al. 1997. Equilibrium responses of global net primary production and carbon storage to doubled atmospheric carbon dioxide: Sensitivity to changes in vegetation nitrogen concentration. — Global Biogeochem. Cycles, v. 11, p. 173 — 189.

Molau U. 1997. Phenology and Reproductive Success in Arctic Plants: Susceptibility to Climate Change. — In: Global Change and Arctic Terrestrial Ecosystems. — Springer-Verlag, New York, p. 153 — 170.

Myneni R. B., Keeling C. D., Tucker C. J., Asrar G., Nemani R. R. 1997. Increased plant growth in the northern high latitudes from 1981 — 1991. — Nature, v. 386, p. 698 — 702.

Oechel W. C., Vourlitis G. L., Hastings S. J., Bochkarev S. A. 1995. Change in Arctic CO_2 flux over two decades: Effects of climate change at Barrow, Alaska. — Ecol. Appl., No. 5, p. 846 — 855.

Payette S., Gagnon R. 1985. Late Holocene deforestation and tree regeneration in the forest-tundra of Quebec. — Nature, v. 313, p. 570 — 572.

Randerson J. T., Field C. B., Fung I. Y., Tans P. P. 1999. Increases in early season ecosystem uptake explain changes in the seasonal cycle of atmospheric CO_2 at high northern latitudes. — Geophys. Res. Let., v. 26, p. 2765 — 2769.

Richards J. A. 1993. Remote Sensing Digital Image Analysis. — Springer-Verlag, 340 p.

Richter D., Kasischke E. S., O'Neill K. P. 1999. Postfire Stimulation of Microbial Decomposition in Black Spruce (Picea mariana L.) Forest Soils: A Hypothesis. — In: Fire, Climate Change and Carbon Cycling in the Boreal Forest, eds. Kasischke E. S., Stocks B. J. — Springer-Verlag, New York, p.197 — 213.

Rosenfield G. H., Fitzpatric-Lins K. 1986. A Coefficient of Agreement as a Measure of Thematic Classification Accuracy. — Photogr. Eng. And Rem. Sensing, v. 52, No. 2, p. 223 — 227.

Shiyatov S. G. 1969. Snowpack on the upper forest border and its impact on the forest. — In: A new data on the Ural flora and vegetation. — Sverdlovsk, p. 141 — 157. (In Russian).

Starfield A. M., Chapin F. S. III. 1996. A dynamic model of arctic and boreal vegetation change in response to global changes in climate and land-use. — Ecol. Appl., v. 6, p. 842 — 864.

Tikhomirov B. A. 1967. Problems of forest-tundra studies. — In: Forest-tundra vegetation. — Leningrad, Nauka, p. 5 — 11 (In Russian).

USSR forests. 1969. Vol. 4. — Moscow: Nauka, 768 p. (In Russian).

Vaganov E. A., Hughes M. K., Kirdyanov A. V., Schweingruber F. H., Silkin P. P. 1999. Influence of snowfall and melt timing on tree growth in subarctic Eurasia. — Nature, v. 400, p. 149 — 151.

Vaganov E. A., Shiyatov S. G., Mazepa V. S. 1996. Dendroclimatic Study in Ural-Siberian Subarctic. — Novosibirsk: Nauka, 246 p. (In Russian).

Van Genderen J. L., Lock B. F., Vass P. A. 1978. Remote Sensing: Statistical Testing of Thematic Map Accuracy. — Remote Sensing of Environment, No. 7, p. 3 — 14.

Zimov S. A., Davidov S. P., Voropaev Y. V. et al. 1996. Siberian CO_2 efflux in winter as a CO_2 source and cause of seasonality in atmospheric CO_2. — Clim. Change, v. 33, p. 111 — 120.

Zimov S. A., Davidov S. P., Zimova G. M., Davidova A. I. et al. 1999. Contribution of Disturbance to Increasing Seasonal Amplitude of Atmospheric CO_2. — Science, v. 284, p. 1973 — 1976.